Magnetic and spectroscopic studies of iron and manganese complexes

Tchouka, Héloïse

CHAPTER 5

Relating the Electrochemical and Vibrational Properties of Mn-tmtacn Complexes to their Catalytic Activity and Selectivity in the Oxidation of Alkenes

The goal of this chapter is to investigate further whether the apparent relation between sterics/selectivity and electronics/activity proposed earlier is indeed valid. Substituted benzoic acids offer an excellent opportunity to clarify correlations made earlier between physical properties and catalytic activity and selectivity in terms of the electron deficiency of the carboxylato ligands employed.

5.1- Introduction

Binuclear Mn-tmtacn complexes (tmtacn = *N,N′,N″*,-trimethyl-1,4,7-triazacyclononane) were first reported by Wieghardt and coworkers in 1985.[1] The chemistry and the industrial application of these complexes have attracted considerable interest not only because of their bleaching activity[2] but also due to their activity as catalysts, for a wide range of selective organic oxidative transformations.[3,4,5] The Mn^{III}-tmtacn complexes, *e.g.* **1**, can either be isolated following spontaneous self-assembly[6] from an ethanolic solution containing manganese(III) acetate, sodium acetate and tmtacn as a tridentate capping ligand, at each of the two Mn(III) ions; or from the reaction of $[Mn^{IV}(O)_3(tmtacn)_2]^{2+}$ (**2**) with a carboxylic acid in the presence of L-ascorbic acid as reducing agent. The carboxylic acid acts as a ligand and substitutes the μ-oxo ligands during the reaction to produce **1**, as shown in the scheme 5.1.

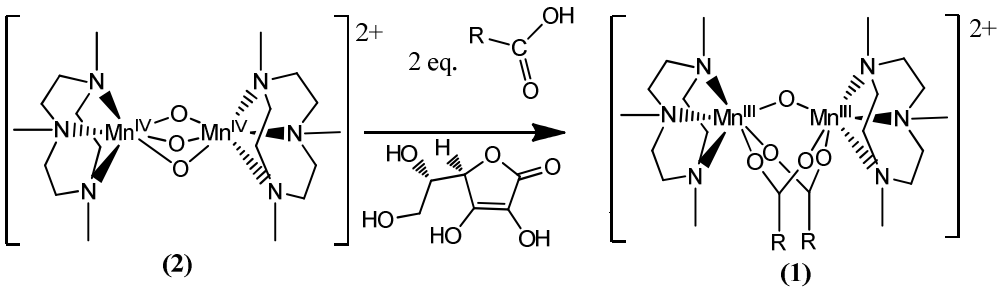

Scheme 5.1: Reaction of $[Mn^{IV}(O)_3(tmtacn)_2]^{2+}$ (**2**) with a carboxylic acid and L-ascorbic acid to form a binuclear catalyst **(1)**.

In the presence of hydrogen peroxide and with a carboxylic acid or other additives, the Mn-tmtacn complexes can catalyze the oxidation of alkenes.[7] During the catalyzed oxidation of organic substrates by **2**, the complex is activated such that the two metal ions will change their oxidation state from the IV-IV to the III-III state; which is accompanied by substitution of two μ-oxo ligands by two μ-carboxylato ligands. A mechanism for the oxidation of alkenes was proposed (Scheme 5.2) in which the addition of the hydrogen peroxide leads to the formation of an initial *bis*-carboxylato species followed by formation of the peroxo species, which then reacts to form either epoxide or *cis*-diol products. The selectivity and activity of these catalysts for either the epoxide or the *cis*-diol product has been investigated in our group,[4,5] and two important conclusions were drawn: i) the activity is mainly dependent on the electron withdrawing properties of the carboxylate and ii) the selectivity is dependent on steric factors.

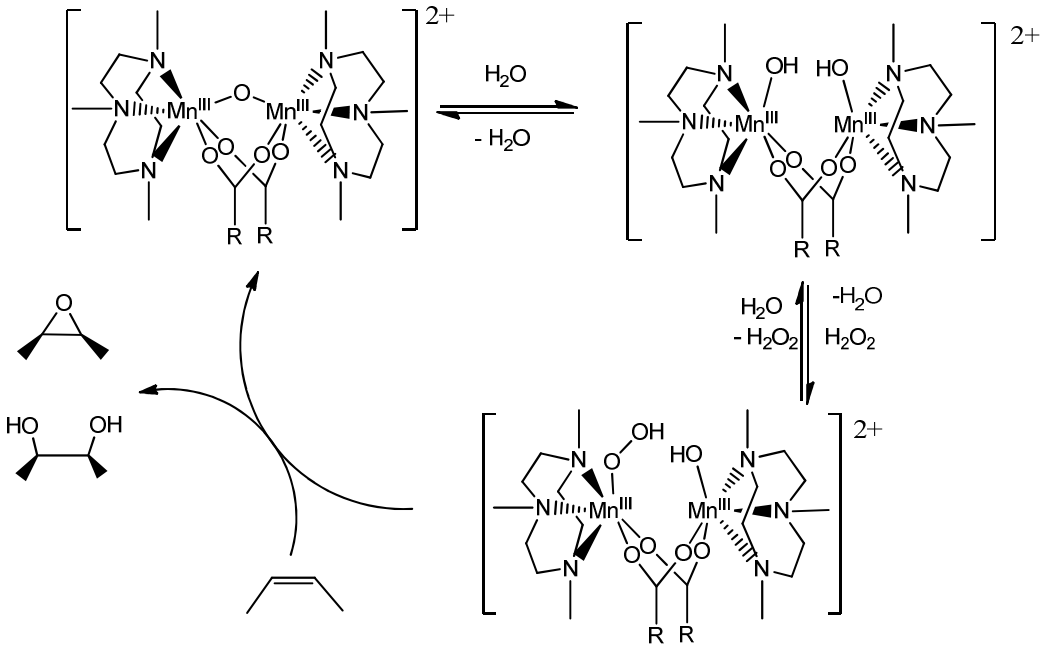

Scheme 5.2: Catalytic cycle for the epoxidation and *cis*-dihydroxylation of alkenes by the family of complexes (**1**).[8]

The carboxylato ligand bridges the two metal centers and a series of such substituted R-carboxylato manganese(tmtacn) were synthesized with R = alkyl, alkylhalide or (substituted) phenyl. This included a series of μ-benzoato complexes, which have been characterized by electrochemistry and for catalytic activity.

The goal of this chapter is to investigate further whether the apparent relation between sterics/selectivity and electronics/activity proposed earlier is indeed valid.[5,7] The substituted benzoic acids offer an excellent opportunity to seek further correlations between physical properties and catalytic activity and selectivity in terms of the electron deficiency of the carboxylato ligands employed.

The effects of variously substituted benzoic acid derivatives on the complex will be investigated in order to determine what correlation, if any, there exists with catalytic activity, which would be useful for tuning of the catalysts. Several of these complexes were synthesized and characterized using FT-IR, UV-Vis, and paramagnetic ^{1}H-NMR spectroscopies. Identification of the manganese-carboxylato band by FT-IR spectroscopy was carried out using isotope labeling and a relation between the carboxylate symmetric and asymmetric stretching modes with redox and catalytic properties investigated.

5.2- Experimental section

5.2.1- Synthesis

All reagents were obtained from commercial sources and used as received unless stated otherwise. Solvents for spectroscopy were of UVASOL grade or better. Complexes **3**-**13** and **15**-**26** studied in this chapter were synthesized according to procedures reported by and were provided by Dr. de Boer.[5]

$[Mn^{III}_2(\mu\text{-}O)(\mu\text{-}4\text{-cyanobenzoato})_2(tmtacn)_2](PF_6)_2$ (**14**) was prepared by the general procedure reported by de Boer et al..[8] 162 mg (0.20 mmol) of $[Mn^{III}_2(\mu\text{-}O)_3(tmtacn)_3](PF_6)_2$ was dissolved in 20 ml of water in a Greiner tube. 65 mg (0.44 mmol) of 4-cyanobenzoic acid dissolved in a minimum amount of water was added to the red solution followed by 38 mg (0.216 mmol) of L-ascorbic acid dissolved in 2 ml water. Upon addition of the ascorbic acid a purple precipitate began to form immediately. The mixture was shaken vigorously for 1-1.5 min. The red-purple precipitate was isolated by filtration and washed three times with diethyl ether. The product was recrystallized by slow diffusion of diethyl ether into acetonitrile. The yield was 65% (232 mg, 0.22 mmol). *Anal Calc* of $[C_{34}H_{50}Mn_2N_8O_5P_2F_{12}]$: C, 38.87%; H, 4.80%; N, 10.67%. Found: C, 38.48%; H, 4.87%; N, 10.60%.

5.2.2- Physical measurements

^{1}H NMR spectra (400.0 MHz) spectra were recorded on a Varian Mercury Plus. Chemical shifts are with respect to the solvent peak (^{1}H NMR spectra CD_3CN: 1.94 ppm). Elemental analyses were performed with a Foss-Heraeus CHN-O-Rapid or a EuroVector Euro EA elemental analyzer. Electrochemical measurements were carried out on a model 630B Electrochemical Workstation (CH Instruments). Analyte concentrations were typically 0.5-1.0 mM in anhydrous acetonitrile containing 0.1 M potassium or tetrabutylammonium hexafluorophosphate (KPF_6 or $(TBA)PF_6$). Unless stated otherwise, a Teflon-shrouded glassy carbon working electrode (CH Instruments), a Pt wire auxiliary electrode, and an SCE or Ag/AgCl reference electrode were employed. Cyclic voltammograms were obtained at sweep rates between 1 mV/s and 10 V/s. For reversible processes, the half-wave potential values are reported. Redox potentials are reported ±10 mV. UV/Vis

absorption spectra were recorded on a Specord600 (JA) spectrophotometer using 10 mm path length quartz cuvettes. FT-IR spectra were recorded using ZnSe/Diamond UATR attachment on a Perkin-Elmer Spectrum400 FT-IR spectrophotometer with a liq. N_2 cooled MCT detector. Raman spectra of solids (4 cm^{-1} resolution) were recorded using a Perkin Elmer Spectrum400 Raman station (at 785 nm).

5.3- Results and discussion

Complex **14** was isolated from an aqueous solution containing $[Mn^{III}_2(\mu\text{-}O)_3(tmtacn)_3](PF_6)_2$, 4-cyanobenzoic acid and L-ascorbic acid and recrystallized from acetonitrile by slow diffusion of ethyl acetate. In this chapter, **14** is studied and used to compare with data available for related complexes reported elsewhere.

5.3.1- Paramagnetic ^{1}H-NMR spectroscopy of 14

The ^{1}H-NMR spectrum of **14** is based on the assignment by Hage and coworkers, derived from deuterium labeling studies.[6] Figure 5.1 shows the labeling convention used for the tmtacn ligand and in figure 5.2 the ^{1}H-NMR spectrum of the *p*-cyanobenzoato complex is shown. Hage et al. reported signals at -96 and 67 ppm that disappear when the methyl groups on the tacn ligand are deuterated, so these are assigned to the methyl groups. One of these methyl groups is oriented *trans* to the oxo group, yielding the signal at -96 ppm, the other two methyl groups are oriented *cis*, and their signals are found at 67 ppm. For the –CH_2 groups in the ligand, a and b are oriented *trans* towards the oxo groups, giving signals at -91 for proton a and -79 ppm for proton b, due to protons b, d and e being 'axial' and more deshielded than the 'equatorial' a, c and f. For the same reason, d and e are assigned to the signals at 68 and 34 ppm, and c and f to 19 and 34 ppm.

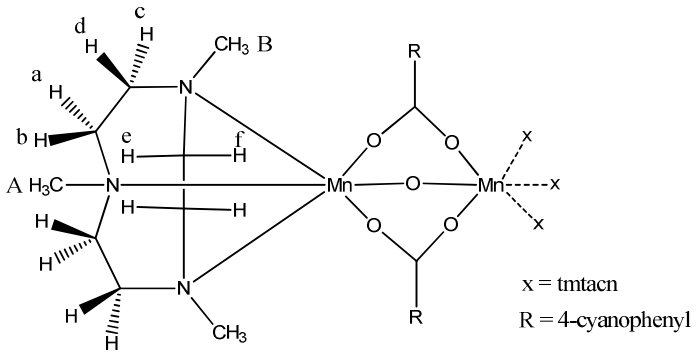

Figure 5.1: Schematic representation of the tmtacn ligand coordinated to manganese.

In the similar manner, signals are assigned as follows for the -CH_3 groups δ -99 (6H, A) and δ 71 (12H, B) and for the -CH_2 groups: δ -92 (4H, a), δ -80 (4H, b), δ 19 (4H, c), δ 34 (8H, e,f) and δ 68 (4H, d), and δ 7.2 (8H, benzoic acid substituents). Note that some signals have shifted compared to the complex described by Hage,[13] due to differences in the electron withdrawing/donating character of the carboxylic acid ligands being used (*vide infra*).

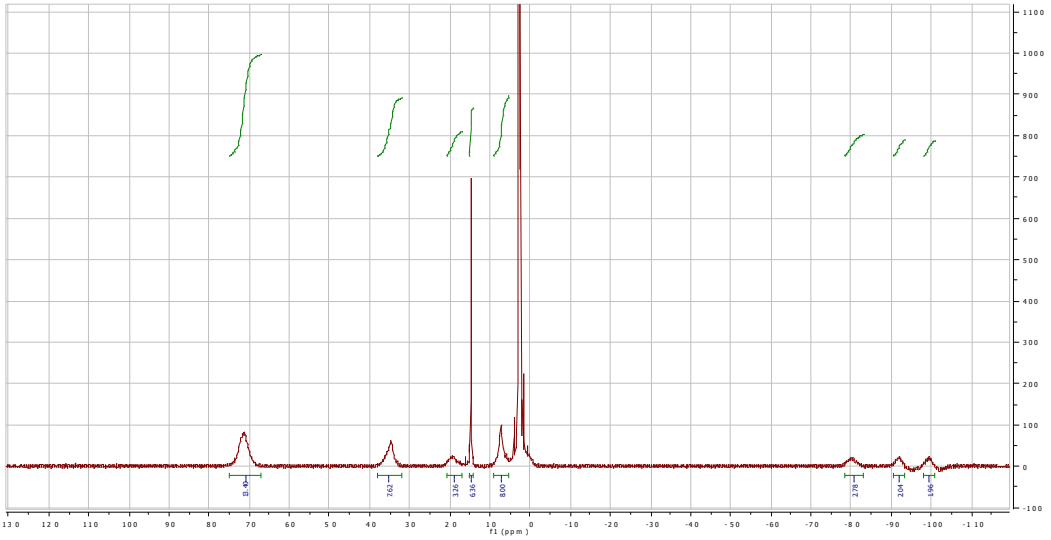

Figure 5.2: Paramagnetic ^{1}H-NMR spectrum of **14**.

5.3.2- Description of the single crystal X-ray structures

Single crystal X-ray structures have been previously determined for a number of the complexes $[Mn^{III}_2(\mu\text{-}O)(\mu\text{-}CCl_3CO_2)_2(tmtacn)_2](PF_6)_2$ (**3**), $[Mn^{III}_2(\mu\text{-}O)(\mu\text{-}CH_3CO_2)_2(tmtacn)_2](PF_6)_2$ (**4**) and $[Mn^{III}_2(\mu\text{-}O)(\mu\text{-benzoato})_2(tmtacn)_2](PF_6)_2$ (**6**).[7,9,12] The structures of complexes $[Mn^{III}_2(\mu\text{-}O)(\mu\text{-4-bromobenzoato})_2(tmtacn)_2](PF_6)_2$ (**8**) and $[Mn^{III}_2(\mu\text{-}O)(\mu\text{-4-nitrobenzoato})_2(tmtacn)_2](PF_6)_2$ (**11**) were reported by de Boer[5] and are shown below (Figure 5.3).

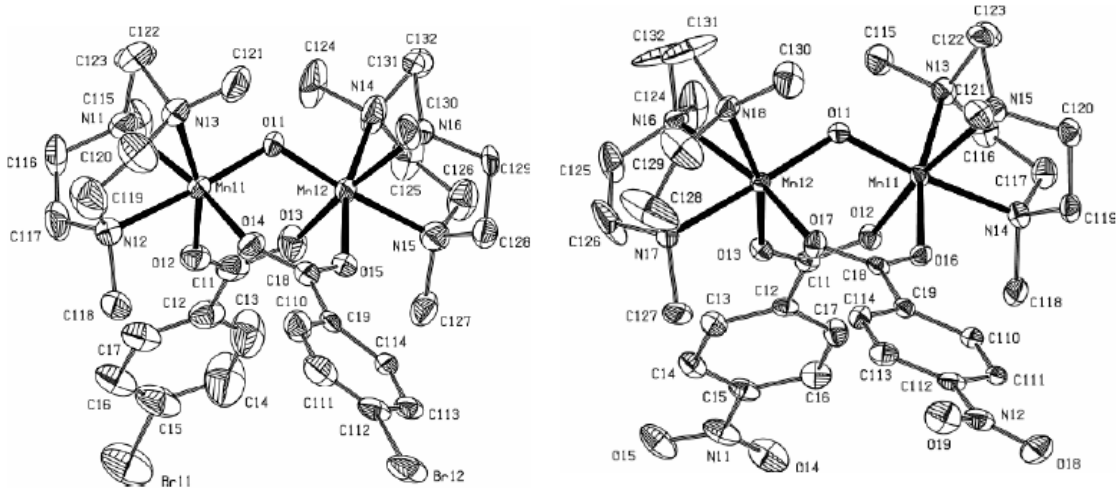

Figure 5.3: Molecular structure of **8** (4-bromobenzoato-Mn complex) (left) and **11** (4-nitrobenzoato-Mn complex) (right) (Ortep drawing). PF_6^- anions were omitted for clarity.

The crystals of **8** have a monoclinic unit cell with eight molecules per unit cell. The formula unit consists of three moieties: one cationic unit $[Mn_2(\mu\text{-}O)(\mu\text{-}4\text{-}Br_2\text{-}benzoato)_2(tmtacn)_2]^{2+}$ complex and two hexafluorophosphate anions. Both metal centers are in similar environment and each metal is coordinated to a capping tmtacn ligand and are coordinated to each other through an oxo ligand and two carboxylato groups. Each manganese atom is in a distorted octahedral environment with the deviation from 90° varying between -10.2 and +6.9°. Each Mn^{3+} ion is facially coordinated to the three nitrogens of tmtacn, one μ-oxo ligand and two μ-carboxylato ligands. The average of Mn-O (oxo) bond length is 1.81(4) Å whereas the Mn-O (carboxlato) is 2.04(5) Å and Mn-N bond length is 2.12(6) Å if the N is in *trans* position to O (oxo) (N-Mn-O_{oxo}) and is somewhat longer, 2.22 Å (6), for the N *trans* to the O of carboxylato ligand (N-Mn-$O_{carboxylato}$). This is ascribed to a *trans*-effect of the carboxylato group on the tmtacn ligand. Complex **11**, crystallized in the monoclinic space group *C2/c*. The formula also consists of one dimeric cation $[Mn_2(\mu\text{-}O)(\mu\text{-}4\text{-}NO_2\text{-benzoato})_2(tmtacn)_2]^{2+}$ and two hexafluorophosphate anions. As for **8**, the metal centers of **11** are in a distorted octahedral environment and the average bond lengths are, 1.81 Å (2) and 2.06 Å (3), respectively, for Mn-O (oxo) and Mn-O (carboxylato) whereas the average bond lengths of Mn-N are 2.13 Å (3) and 2.23 Å (3), respectively, for N-Mn-O_{oxo} and N-Mn-$O_{carboxylato}$. The Mn-O (oxo) shows a characteristic bond length typical for the Mn-O-Mn entity[10,11] and is in agreement with that reported for $[Mn_2(\mu\text{-}O)(\mu\text{-benzoato})_2(tmtacn)_2]^{2+}$ (**6**).[7] The above mentioned Mn-

N (N-Mn-$O_{carboxylato}$) bond lengths appear to be longer compared to that reported for $[Mn_2(\mu\text{-}O)(\mu\text{-}CCl_3COO)_2(tmtacn)_2]^{2+}$ (**3**) (2.19 Å (7)),[12] which could be due to the *trans*-effect from the aryl carboxylate group. Possibly reflecting steric differences between the benzoato ligands compared to the (trichloro)acetato ligands, a decrease of the Mn-O-Mn bond angle from 125-126° to 121-123°, respectively, is observed for μ-CCl_3COO (**3**)/μ-CH_3COO (**4**) and μ-benzoato complexes. Table 5.1 shows a comparison of selected bond lengths for **3**, **4**, **6**, **8** and **11**.

Table 5.1 Selected interatomic distances (Å) and bond angles (deg.) of **3**, **4**, **6**, **8** and **11**.

	μ -CH_3COO	μ-CCl_3COO	μ-benzoato	μ-4-Br-benzoato	μ-4-NO_2-benzoato
Mn-O_{oxo} (Å)	1.83(6)	1.80(13)	1.81(13)	1.81(4)	1.81(4)
Mn-O_{carbox} (Å)	1.96(6)	2.09(15)	2.05(14)	2.05(5)	2.07(2)
Mn-$N_{(trans\text{-}oxo)}$ (Å)	2.13(6)	2.12(17)	2.12(16)	2.13(6)	2.13(3)
Mn-$N_{(trans\text{-}carbox)}$ (Å)	2.12(8)	2.20(17)	2.23(16)	2.22(6)	2.23(3)
Mn-O-Mn (°)	125.1(3)	125.9(7)	121.78(8)	121.0(2)	122.6(12)

5.3.3- Cyclic voltammetry of 14

The cyclic voltammogram (CV) of **14** in acetonitrile in the potential range -0.4 to +1.6 V is shown in figure 5.4. As for most of the complexes, it shows a reversible one-electron oxidation at $E_{1/2}$ 0.94 V (with Ag/AgCl reference electrode), which corresponds to 1.16 V (*vs* SCE) assigned to the redox couple $Mn^{III}{}_2/Mn^{III,IV}{}_2$. A reversible one-electron reduction is observed at $E_{1/2}$ = -0.19 V, which corresponds to the $Mn^{III}{}_2/Mn^{II,III}{}_2$ redox couple.

$$[Mn^{II}(\mu\text{-}O)(\mu\text{-}RCO_2)_2(tmtacn)_2Mn^{III}] \underset{+e^-}{\overset{-e^-}{\rightleftharpoons}} [Mn^{III}(\mu\text{-}O)(\mu\text{-}RCO_2)_2(tmtacn)_2Mn^{III}] \underset{+e^-}{\overset{-e^-}{\rightleftharpoons}} [Mn^{IV}(\mu\text{-}O)(\mu\text{-}RCO_2)_2(tmtacn)_2Mn^{III}]$$

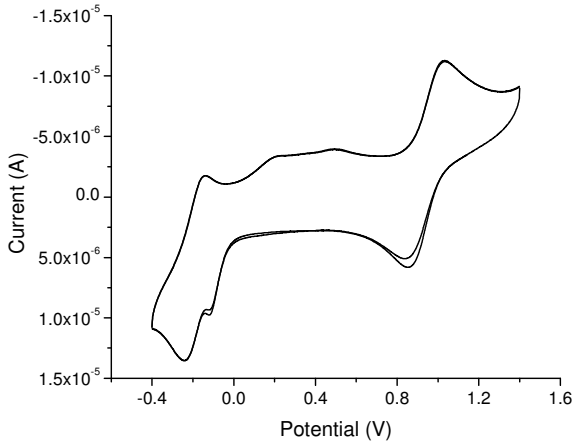

Figure 5.4: Cyclic voltammogram of μ-4-cyanobenzoato complex **14** in CH_3CN, 0.1 M KPF_6, with Ag/AgCl reference electrode and scan rate of 0.1 V/s.

This oxidation and reduction behavior is similar to that reported for $[Mn^{III}_2(\mu\text{-}O)(\mu\text{-}CH_3COO)_2(tmtacn)_2]$ by Wieghardt and cowokers.[4] The redox potentials for a series of complexes are summarized in table 5.2 (*vide infra*).

5.3.4- FT-IR and Raman spectroscopy

The Mn-O-Mn modes of $[Mn_2O_3(tmtacn)_2](PF_6)_2$ (**2**) have been assigned to the bands at 701 and 668 cm^{-1} and are shown in figure 5.5.[13] The band at 701 cm^{-1} is weak in the FT-IR spectrum and relatively intense in the Raman spectrum. The overtones bands (1460 and 1293 cm^{-1}) are less intense in Raman compared to the IR spectrum. It would be expected that assignment of the corresponding band in the Raman and IR spectra of **6** could be made using ^{18}O labeling. The $\upsilon Mn\text{-}^{16}O$ and $\upsilon Mn\text{-}^{18}O$ modes are at 664 and 653 cm^{-1}, respectively (Figure 5.6). However since the complex is bearing only one μ-oxo bridge and the polarizability may be less compared to that of **2**, it is difficult to identify these bands in the Raman spectra. In fact the Raman measurements carried out on ^{18}O labeled **6** (Figure 5.7) show only a small difference that is too weak to be conclusive.

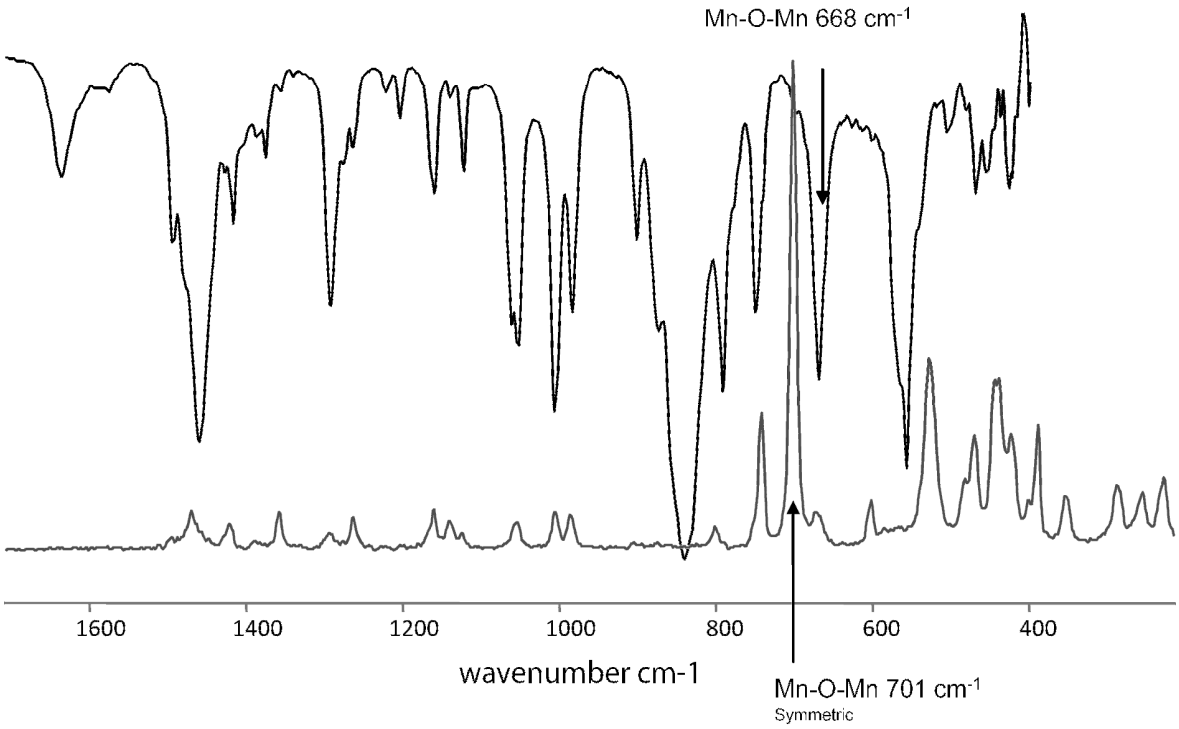

Figure 5.5: (upper) FT-IR and (bottom) Raman spectra of **2**.

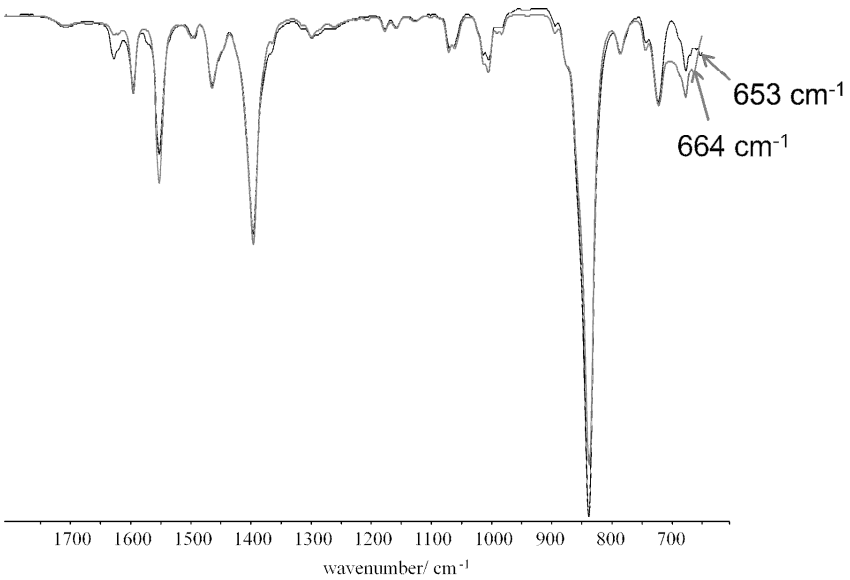

Figure 5.6: FT-IR spectra of carboxylate ^{16}O of **6** (grey) and ^{18}O of **6** (black).

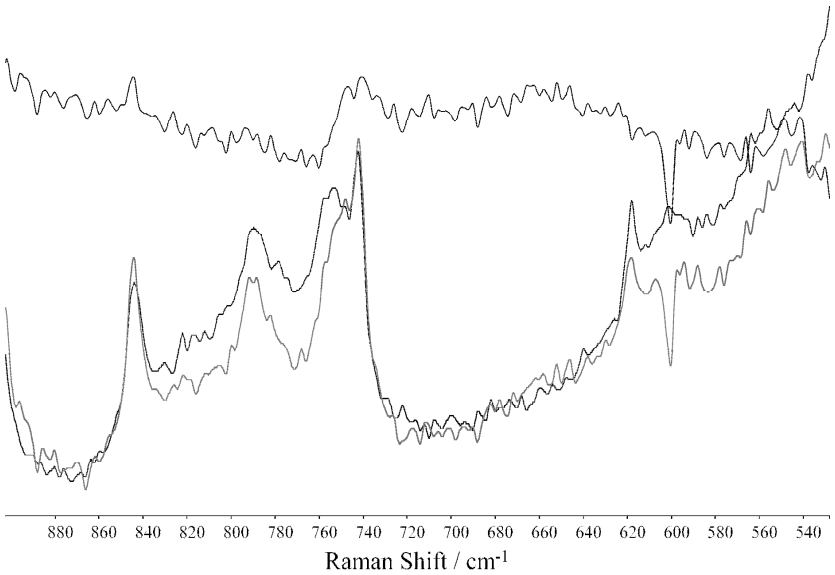

Figure 5.7: Raman spectra of Mn^{III}_2 (μ-^{16}O)(μ-benzoato)$_2$(tmtacn)$_2$](PF$_6$)$_2$ (**6**) (grey) and Mn^{III}_2 (μ-^{18}O)(μ-benzoato)$_2$(tmtacn)$_2$](PF$_6$)$_2$ (black) complexes and the difference (upper line) in acetonitrile.

Although recording a solid state Raman spectra was precluded by burning due to the absorption of laser radiation by the complexes, FT-IR spectroscopy could be employed for determining the effect of ligand variation on the carboxylate vibration modes.

By using ^{13}C-labeled **6** and d_5-phenyl labeled **6**, the C=O and C-O modes could be assigned. Figure 5.8 shows the FT-IR spectra of **6** and ^{13}C-labeled of **6**. The C=O and C-O stretching vibrations of benzoic complex, appearing respectively at 1551 and 1393 cm^{-1} are shifted to 1517 and 1359 cm^{-1} for ^{13}C-labeled of **6**. The FT-IR spectrum of d_5-**6,** also show

isotope shifts in the spectra (see Figure 5.9). However the shift observed in the CO vibration region suggest that these bands are not due to only the carboxylate but are also sensitive to their substituents.

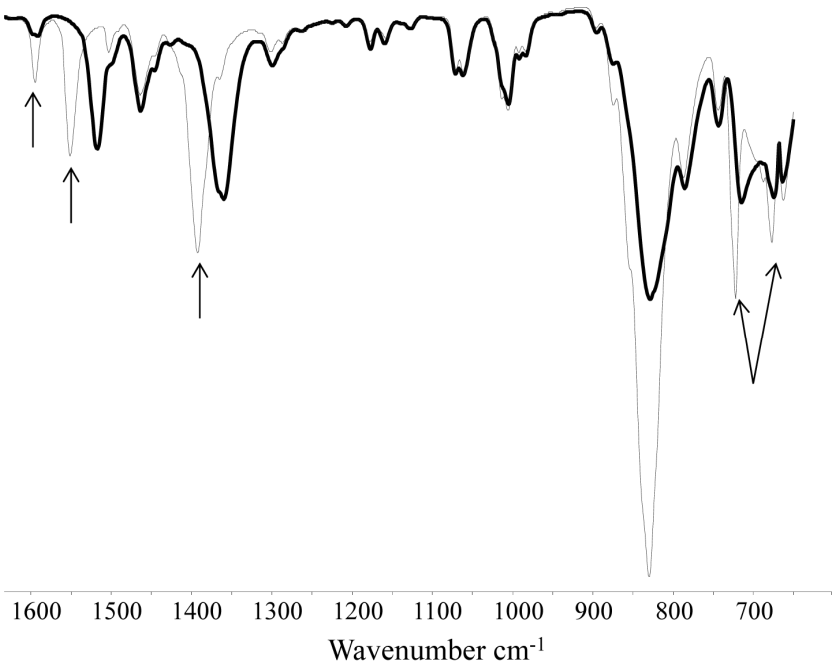

Figure 5.8: FT-IR spectra of Mn^{III}_2 (μ-O)(μ-benzoato)$_2$(tmtacn)$_2$](PF$_6$)$_2$ (**6**) (grey) and Mn^{III}_2 (μ-O)(μ-($^{13}CO_2$)benzoato)$_2$(tmtacn)$_2$](PF$_6$)$_2$ (black) complexes.

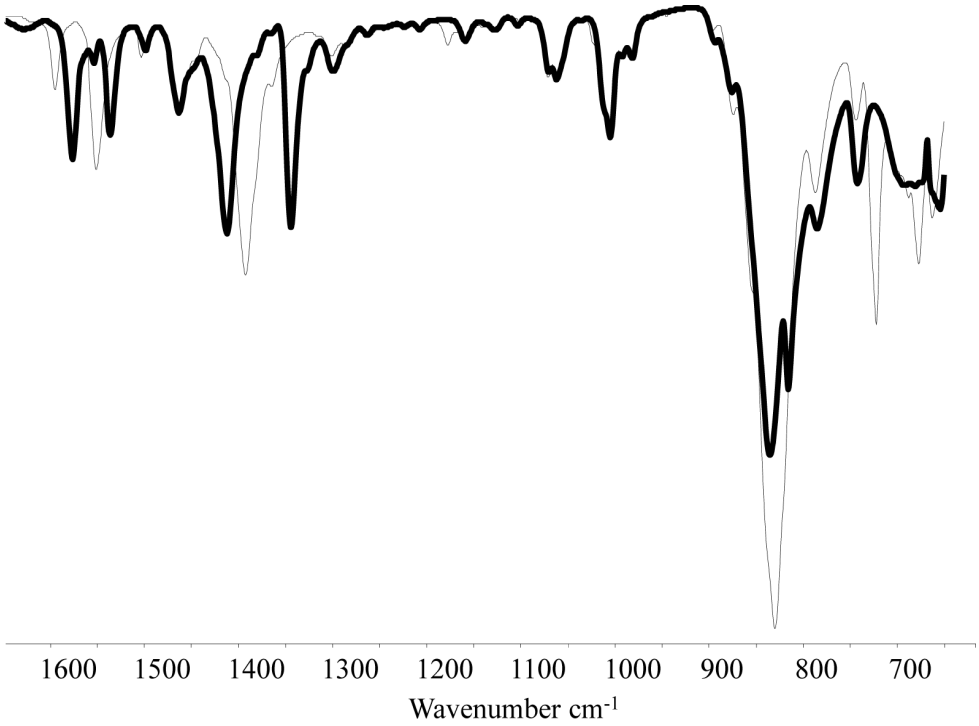

Figure 5.9: FT-IR spectra of natural abundance Mn^{III}_2 (μ-O)(μ-benzoato)$_2$(tmtacn)$_2$](PF$_6$)$_2$ (**6**) (black) and (Mn^{III}_2 (μ-O)(μ-CO$_2$) d$_5$-benzoato)$_2$(tmtacn)$_2$](PF$_6$)$_2$ (**6**) (grey) complexes.

In the Raman spectra of μ-acetato (**4**), μ-trichloro (**3**), and μ-benzoato (**6**) shown in figure 5.10, the carboxylate modes are observed at 1575 and 1428 cm^{-1}, 1660 and 1371 cm^{-1}, 1552 and 1393 cm^{-1}, respectively, for **4**, **3**, and **6**. Although these bands seem to be sensitive to either the steric or electronic properties of the carboxylato substituent, they are however influenced only slightly by the substituent on the benzoato group.

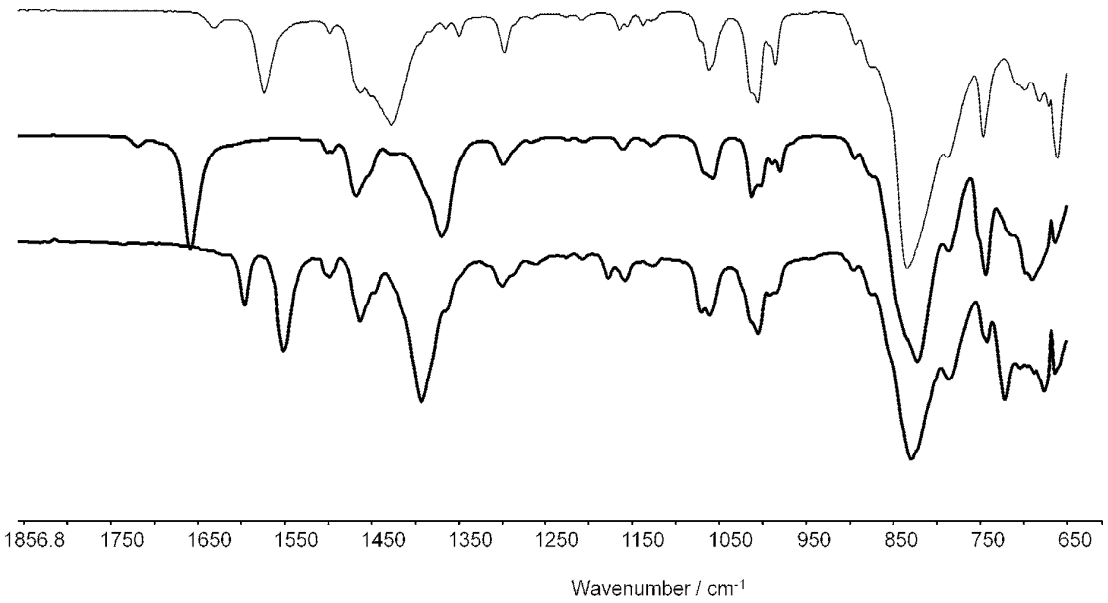

Figure 5.10: FT-IR spectra of μ-acetato (**4**) (dotted lines), μ-trichloro (**3**) (black lines) and μ-benzoato (**6**) (grey lines).

5.3.5- Electronic spectra

The absorption spectra of several *para*-substitued benzoic complexes **6**, **8**, **11**, **13**, **14** recorded in acetonitrile are shown in figure 5.11. In the visible region, the spectra of the different complexes are quite similar and are comparable to that reported earlier.[1] The bands appearing in the region between 480 and 520 nm are assigned to the metal centered / MLCT transitions within the $[Mn_2(\mu\text{-}O)(\mu\text{-}CH_3CO_2)_2]$ core and are similar to those reported for $[Mn^{III}_2(\mu\text{-}O)(\mu\text{-}CH_3CO_2)_2(tmtacn)_2]^{2+}$;[14,15] on the basis that the corresponding stretching modes of $Mn_2\text{-}O_2CCH_3$ were reported to be enhanced when excited at 457 and 488 nm.[16] The absorption band at 760 nm is assigned to the d-d transitions for high spin d^4 Mn(III) complexes, which is comparable to that observed for mononuclear Mn(III) compounds.[17] However the increase in intensity of the band at 550 nm seems to be sensitive to the electron withdrawing substituent group; the more electron deficient, the more intense it is.

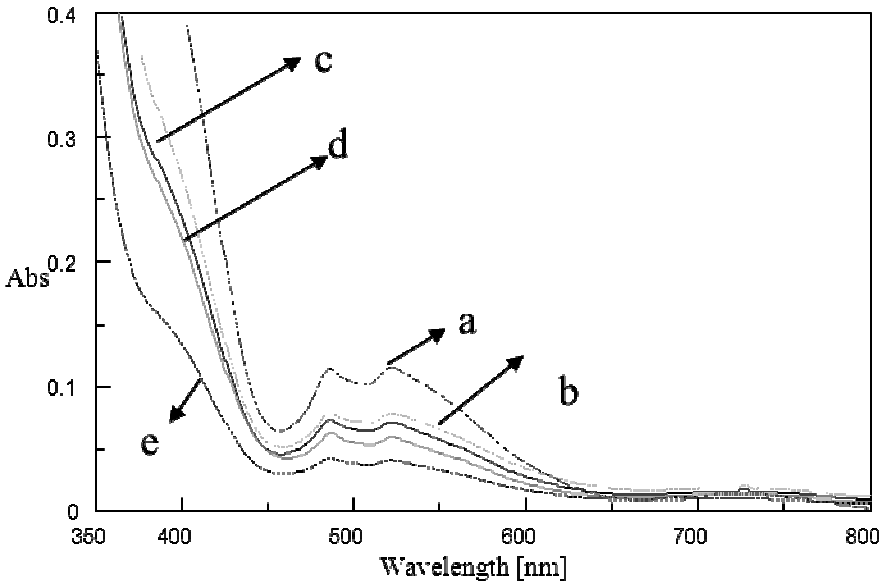

Figure 5.11: UV/Vis spectra of (a) $[Mn^{III}_2(\mu\text{-}O)(\mu\text{-}4\text{-CN-benzoato})_2(tmtacn)_2](PF_6)_2$ (**14**), (b) $[Mn^{III}_2(\mu\text{-}O)(\mu\text{-}4\text{-}NO_2\text{-benzoato})_2(tmtacn)_2](PF_6)_2$ (**11**), (c) $[Mn^{III}_2(\mu\text{-}O)(\mu\text{-benzoato})_2(tmtacn)_2](PF_6)_2$ (**6**), (d) $[Mn^{III}_2(\mu\text{-}O)(\mu\text{-}4\text{-}CH_3O\text{-benzoato})_2(tmtacn)_2](PF_6)_2$ (**13**) and (e) $[Mn^{III}_2(\mu\text{-}O)(\mu\text{-}4\text{-Br-benzoato})_2(tmtacn)_2](PF_6)_2$ (**8**).

Table 5.2 shows the oxidation potentials of a series of $[Mn_2(\mu\text{-}O)(\mu\text{-}RCO_2)_2(tmtacn)_2]^{n+}$ complexes. The differences observed in the potential values for each complex are due to the different μ-carboxylic ligands used. Apart from the μ-acetato complex for which the $E_{1/2}$ ($Mn^{III}_2/Mn^{III,IV}_2$) is less than 1 V, the rest of the substituted carboxylato complexes have a redox potential greater or equal to 1 V with the highest value being for the μ-trichlorocarboxylato complex (1.40 V). The μ-benzoato complex shows a $E_{1/2}$ of 1.06 V, which is similar to that observed for its analogs with the exception of **11** (the *para*-NO_2 substituted benzoato complex). However, the redox potential increases for di- and tri-substituted benzoato complexes. From FT-IR spectroscopy, the carboxylate modes also show differences from each other except for the band at around 1400 cm^{-1} for benzoato and its substituents complexes which is quite similar and this band is assigned to the O-C-O vibration. The insensitivity of this band is probably due to the fact that it is related to the angle between O-C-O bonds, and this angle seems to be the same for benzoate and substituted benzoate complexes (Table 5.1).

Although it was previously observed[8] that the *ortho*-, *meta*- and *para*-mono substituted benzoate complexes show differences in activity and not with *cis*-diol/epoxide

selectivity (see table 5.3), these however, are not reflected in their redox potentials. There are in fact no trends observed between redox potentials and activity/selectivity of various substituted benzoic acid complexes.

Table 5.2 Redox data and carboxylato modes of a series of $[Mn_2(\mu\text{-}O)(\mu\text{-}RCO_2)_2(tmtacn)_2]^{n+}$ complexes.[a]

Complex	RCO_2^-	CV $E_{½}$ III,III-III,IV	ref	IR (this chapter) C-O, O-C-O (cm^{-1})
3	$CCl_3CO_2^-$	1.40 (120)	5	1659, 1368
4	$CH_3CO_2^-$	0.98 (120)	5	1574, 1428
5	$^-O_2C(CH_2)_3CO_2^-$	1.05 (155)	5	1570, 1399
6	benzoato	1.06 (90)	7	1551, 1393
7	4-iodobenzoato	1.08 (95)	5	1546, 1399
8	4-bromobenzoato	1.09 (100)	5	1551, 1399
9	4-chlorobenzoato	1.10 (95)	5	
10	4-fluorobenzoato	1.08 (105)	5	1560, 1399
11	4-nitrobenzoato	1.15 (80)	5	1521, 1404
12	4-hydroxybenzoato	1.01 (130)	8	
13	4-methoxybenzoato	1.03 (110)	7	1541, 1385
14	4-cyanobenzoato	1.16	This chapter	1553, 1395
15	3-chlorobenzoato	1.15 (110)	8	1560, 1397
16	3-hydroxybenzoato	1.07 (95)	7	1561, 1392
17	3-cyanobenzoato	1.17 (99)	5	1570, 1401
18	3,5-difluorobenzoato	1.15 (120)	8	1572, 1389
19	3,4-difluorobenzoato	1.11 (80)	8	1569, 1385
20	2,4-difluorobenzoato	1.11 (90)	8	1609, 1384
21	2,6-difluorobenzoato	1.16 (130)	8	1599, 1402
22	2,6-dichlorobenzoato	1.24 (100)	8	1589, 1387
23	2,4-dichlorobenzoato	1.16 (100)	8	1551, 1391
24	2,4,6-trichlorobenzoato	1.25 (170)	9	1586, 1387
25	2,4,6-trimethylbenzoato	1.19 (173)	8	
26	2-methoxybenzoato	1.00 (95)	7	1551, 1377

[a] All complexes are 1 mM in CH_3CN (0.1 M $TBAPF_6$ or KPF_6), scan rate 100 mVs^{-1}. $E_{½}$ in V vs. SCE or Ag/AgCl ($|E_{p,a}\text{-}E_{p,c}|$ in mV). For irreversible processes only $E_{p,c}$ or $E_{p,a}$ is given. All values +/-10 mV. (ref = reference)

Table 5.3: *Cis*-dihydroxylation and epoxidation of cyclooctene by some complexes (from ref 8)

complexes	T.O.N		Mass balance (%)
	cis-diol	epoxide	
benzoato	110	60	96
2-chlorobenzoato	165	80	96
3-chlorobenzoato	253	113	98
4-chlorobenzoato	88	42	97
2-methoxybenzoato	244	158	93
4-methoxybenzoato	137	83	96
2-hydroxybenzoato	225	320	90
3-hydroxybenzoato	260	325	89
4-hydroxybenzoato	219	170	93

T.O.N = turn over numbers

5.4- Conclusion

A series of binuclear complexes of the type $[Mn^{III}(\mu\text{-oxo})(\mu\text{-}RCO_2)_2(tmtacn)_2Mn^{III}]$ (with R = alkyl, alkylhalide or (substituted) phenyl group) have been studied. The crystal structures of these complexes confirm the coordination of each manganese ion to the tridentate *N*, *N'*, *N''*-trimethyl-1,4,7-triazacyclononane capping ligand and the triple coordination of both manganese ions to each other through an oxo and two carboxylato ligand. Although the use of benzoic acid results in a decrease of the Mn-O-Mn angle compared to the acetic acid, substitution of the benzoic acid at *para*-position did not have any further effect on the angle, despite differences in the electronic properties. The analysis of spectroscopic and electronic properties of this series of complexes does not show a relation between redox potential and catalytic activity. Although in general it was noted that the activity of these complexes increase with the increase in the electron-withdrawing character of the carboxylate used,[8] activity increases with the electron-donating character of the *para*-substituent of the benzoic acid used also (*i.e.* as shown in table 5.3, μ-4-hydroxo > μ-4-methoxy > μ-4-chloro). Hence redox potential is not of useful as a predictor and neither do the complexes show trends between modes in the FT-IR spectra and catalytic activity. Therefore it is apparent that contrary to earlier conclusions,[8] it is in fact not possible to predict the catalytic activity of these complexes from their redox potentials (*i.e.* the electron withdrawing/donating character of the carboxylato ligand). These data suggest that the electronic effect of the carboxylato ligands is composed of two or more contributions which affect the ability of the Mn-O-Mn bonding to be broken and allow H_2O_2 to coordinate.

5.5- References

1. Wieghardt, K.; Bossek, U.; Ventur, D.; Weiss, J., *J. Chem. Soc., Chem. Commun.,* **1985**, 347.
2. (a) Hage, R.; Lienke, A., *J. Mol. Catal. A: Chem.*, **2006**, *251*, 150. (b) Hage, R.; Lienke, A., *Angew. Chem., Int. Ed.,* **2006**, *45*, 202.
3. Hage, R., *Recl. Trav. Chim.* Pays-Bas, **1996**, *115*, 385.
4. Browne, W. R.; de Boer, J. W.; Pijper, D.; Brinksma, J.; Hage, H.; Feringa, B. L., Manganese-Catalysed Oxidation with hydrogen Peroxide, in: Modern Oxidation Methods, J.-E. Bäckvall (ed.), Wiley-VCH, Weinheim, **2010**, 371.

5. De Boer, J. W., cis-Dihydroxylation and Epoxidation of Alkenes by Manganese Catalysts. PhD thesis, **2008**, University of Groningen.

6. Wieghardt, K.; Bossek, U.; Ventur, D.; Weiss, J., *J. Chem. Soc., Chem. Commun.,* **1985**, 347.

7. de Boer, J. W.; Alsters, P. L.; Meetsma, A.; Hage, R.; Browne, W. R.; Feringa, B. L., *Dalton Trans.,* **2008**, 6283.

8. de Boer, J. W.; Browne, W. R.; Brinksma, J.; Alsters, P. L.; Hage, R.; Feringa, B. L., *Inorg. Chem.*, **2007**, *46*, 6353.

9. Wieghardt, K.; Bossek, U.; Nuber, B.; Weiss, J.; Bonvoisin, J.; Corbella, M.; Vitols, S. E.; Girerd, J. J., *J. Am. Chem. Soc.*, **1988**, *110*, 7398.

10. Wieghardt, K.; Ventur, D.; Tsai, Y. H.; Krûger, C., *Inorg. Chim. Acta*, **1985**, *99*, L25.

11. Hagen, K. S.; Westmoreland, T. D.; Scott, M. J.; Armstrong, W. H., *J. Am. Chem. Soc.*, **1989**, *111*, 1907.

12. de Boer J. W.; Brinksma, J.; Browne, W. R.; Meetsma, A.; Alsters, P. L.; Hage, R.; Feringa, B. L., *J. Am. Chem. Soc.*, **2005**, *127*, 7990.

13. Hage, R.; Krijnen, B.; Warnaar, J. B.; Hartl, F.; Stufkens, D. J.; Snoeck, T. L., *Inorg. Chem.,* **1995**, *34*, 4973.

14. Wieghardt, K.; Bossek, U.; Bonvoisin, J.; Beauvillain, P.; Girerd, J.J.; Nuber, B.; Weis, J.; Heinze, J., *Angew. Chem.*, **1986**, *98*, 1026.

15. Bennu, T. H.; Sabne, S.; Deshpande, S. S.; Srinivas, D.; Sivasanker, S., *J. Molecular Catalysis A*: **2002**, *185*, 71.

16. Sheats, J. E.; Czernuszewicz, R. S.; Dismukes, G. C.; Rheingold, A. L.; Petrouleas, V.; Stubbe, J.; Armstrong, W. H.; Beer, R. H.; Lippard, S. J., *J. Am. Chem. Soc.*, **1987**, *109*, 1435.

17. Dingle, R., *Acta Chem. Scand.,* **1966**, *20*, 33.